Receptor-type protein tyrosine phosphatase alpha (PTPα) mediates MMP14 localization and facilitates triple-negative breast cancer cell invasion

Lisa R. Decotret[a,b,c], Brennan J. Wadsworth[a,c], Ling Vicky Li[b,c], Chinten J. Lim[b,c,d], Kevin L. Bennewith[a,c], and Catherine J. Pallen[b,c,d,*]

[a]Integrative Oncology, BC Cancer, Vancouver, British Columbia, BC V5Z 4E6, Canada, [b]Michael Cuccione Childhood Cancer Research Program, BC Children's Hospital Research Institute, Vancouver, British Columbia, BC V5Z 4H4, Canada; [c]Department of Pathology and Laboratory Medicine and [d]Department of Pediatrics, University of British Columbia, Vancouver, British Columbia, BC V6H 3V4, Canada

ABSTRACT **The ability of cancer cells to invade surrounding tissues requires degradation of the extracellular matrix (ECM). Invasive structures, such as invadopodia, form on the plasma membranes of cancer cells and secrete ECM-degrading proteases that play crucial roles in cancer cell invasion. We have previously shown that the protein tyrosine phosphatase alpha (PTPα) regulates focal adhesion formation and migration of normal cells. Here we report a novel role for PTPα in promoting triple-negative breast cancer cell invasion in vitro and in vivo. We show that PTPα knockdown reduces ECM degradation and cellular invasion of MDA-MB-231 cells through Matrigel. PTPα is not a component of TKS5-positive structures resembling invadopodia; rather, PTPα localizes with endosomal structures positive for MMP14, caveolin-1, and early endosome antigen 1. Furthermore, PTPα regulates MMP14 localization to plasma membrane protrusions, suggesting a role for PTPα in intracellular trafficking of MMP14. Importantly, we show that orthotopic MDA-MB-231 tumors depleted in PTPα exhibit reduced invasion into the surrounding mammary fat pad. These findings suggest a novel role for PTPα in regulating the invasion of triple-negative breast cancer cells.**

Monitoring Editor
Carole Parent
University of Michigan

Received: Jan 22, 2020
Revised: Jan 29, 2021
Accepted: Feb 6, 2021

INTRODUCTION

Breast cancer is the second leading cause of death among women and accounts for 25% of new cancer diagnoses (Canadian Cancer Statistics Advisory Committee, 2019). Triple-negative breast cancer (TNBC), a subtype of breast cancer characterized by loss of progesterone receptor (PR), estrogen receptor (ER), and human epidermal growth factor receptor 2 (HER2) expression, accounts for 10–15% of all breast carcinomas (Dawson *et al.*, 2009). Patients diagnosed with TNBC typically have a poor prognosis, since TNBC is non-responsive to traditional hormone therapies and exhibits an increased likelihood of invading the surrounding breast tissue or metastasizing to lymph nodes, bone, liver, or lungs (Al-Mahmood *et al.*, 2018).

Metastasis is a complex multi-step process during which cancer cells invade through the surrounding extracellular matrix (ECM), intravasate into the blood or lymphatic vessels, survive in circulation, and extravasate through the vessel endothelium to colonize secondary sites (Scully *et al.*, 2012; Al-Mahmood *et al.*, 2018). Invasion through the ECM is partially mediated by the formation of protrusive structures (Murphy and Courtneidge, 2011), including invadopodia and podosomes (collectively referred to as "invadosomes") (Paterson and Courtneidge, 2018). These invasive structures are actin-based dynamic protrusions of the plasma membrane that form on the ventral surfaces of cells and represent concentrated areas of proteolytic activity (Murphy and Courtneidge, 2011; Beaty and Condeelis, 2014; Revach and Geiger, 2014). Invadopodia are

This article was published online ahead of print in MBoC in Press (http://www.molbiolcell.org/cgi/doi/10.1091/mbc.E20-01-0060) on February 10, 2021.

Competing interests: The authors declare no potential conflicts of interest.

*Address correspondence to: Catherine Pallen (cpallen@mail.ubc.ca).

Abbreviations used: Cav-1, caveolin-1; ECM, extracellular matrix; EEA1, early endosome antigen 1; MMP, matrix metalloproteinases; PTPα, receptor-type tyrosine-protein phosphatase alpha; TNBC, triple-negative breast cancer.

© 2021 Decotret *et al.* This article is distributed by The American Society for Cell Biology under license from the author(s). Two months after publication it is available to the public under an Attribution–Noncommercial–Share Alike 3.0 Unported Creative Commons License (http://creativecommons.org/licenses/by-nc-sa/3.0).

"ASCB®," "The American Society for Cell Biology®," and "Molecular Biology of the Cell®" are registered trademarks of The American Society for Cell Biology.

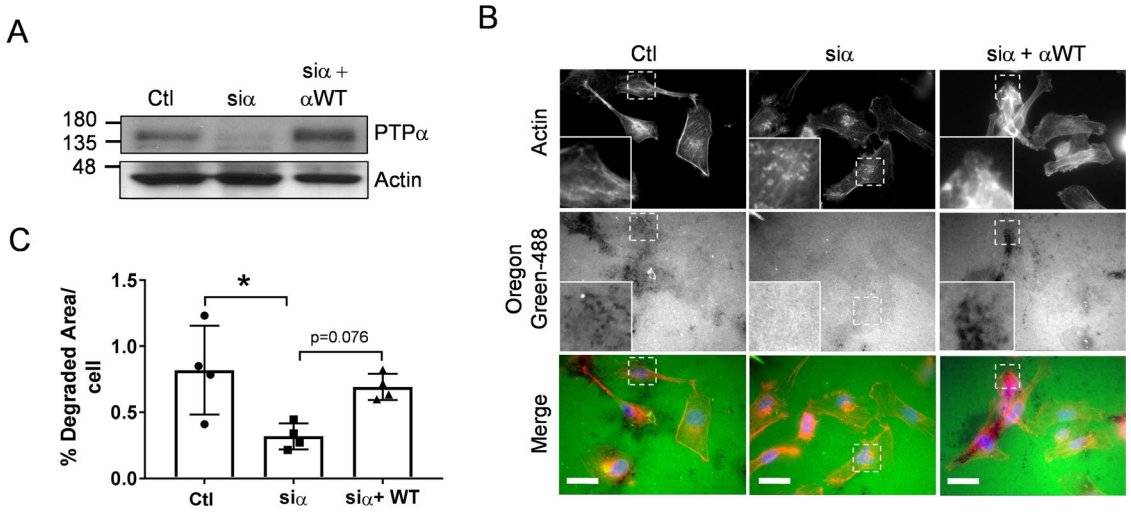

FIGURE 1: Depletion of PTPα reduces extracellular matrix degradation. MDA-MB-231 cells were transfected with nontargeting siRNA (Ctl) or siRNA #1 + #2 (siα) alone or together with siRNA-resistant PTPα-expressing plasmid (αWT). (A) Cell lysates were collected 48 h post siRNA treatment and immunoblotted for PTPα and actin. (B) Cells were plated onto Oregon Green 488-gelatin–coated coverslips for 24 h and stained with DAPI and phalloidin-594 to detect actin. Scale bars = 25 μm. The boxed regions are enlarged in the bottom left corner of each image. (C) The area of degraded matrix per cell per field of view was quantified from four independent experiments as in B, with an average of 80 cells quantified per experiment. Data are mean ± SD ($n = 4$, $*p < 0.01$, one-way ANOVA with Dunnett post hoc analysis).

characterized by the preferential enrichment of matrix metalloproteinases (MMPs), specifically MMP2, MMP9, and MT1-MMP (MMP14), with MMP function and localization to proteolytically active structures being primarily dependent upon endocytic/exocytic trafficking (Yamaguchi *et al.*, 2009; Frittoli *et al.*, 2011). Invadopodia have been studied both in vitro and in vivo and are important for mediating cancer cell intravasation, extravasation and metastasis (Gligorijevic *et al.*, 2012; Leong *et al.*, 2014; Lohmer *et al.*, 2014; Williams *et al.*, 2019). A further understanding of the molecular mechanisms that regulate the formation and function of invasive plasma membrane structures is crucial for the identification of clinically relevant targets to prevent metastasis.

The receptor-type protein tyrosine phosphatase alpha (PTPα) is a widely expressed 130-kDa transmembrane PTP with a short extracellular glycosylated domain and two intracellular catalytic domains (Pallen, 2003). PTPα belongs to the PTP superfamily, which contains over 110 other receptor-type and intracellular PTPs, sharing a high level of homology with the closely related PTPε (Krueger *et al.*, 1990). Other groups have shown that PTPα regulates the invasiveness of colon cancer cells using an ex vivo chicken chorioallantoic membrane (CAM) assay (Krndija *et al.*, 2010). Moreover, PTPα is an activator of the proto-oncogene c-Src and other Src family kinases (SFKs), through dephosphorylation of the regulatory C-terminal tyrosine site (Tyr^{527}) of c-Src in vitro and in vivo (Ponniah *et al.*, 1999; Pallen, 2003). Fibroblasts derived from the embryos of PTPα knockout mice display enhanced Src phosphorylation at Tyr^{527}, accompanied by reduced Src activity (Ponniah *et al.*, 1999; Su *et al.*, 1999). Moreover, these fibroblasts exhibit impaired cell spreading and migration, which is associated with a reduction in focal adhesion (FA) formation (Su *et al.*, 1999; Von Wichert *et al.*, 2003; Zeng *et al.*, 2003). FAs and invasive structures found in cancer cells are remarkably similar structures that share several signaling mechanisms and structural components (Murphy and Courtneidge, 2011; Beaty and Condeelis, 2014; Revach and Geiger, 2014). Indeed, invadopodia formation is initiated by FAs that establish the initial cell-ECM interactions. In invasive cells, Src is released from FAs and localized to invadopodia, which then leads to the recruitment of other key invadopodia components required for formation, maturation and function (Spinardi *et al.*, 2004; Chan *et al.*, 2009; Mader *et al.*, 2011). Because PTPα has been shown to regulate FA formation and cellular migration and due to the similarities between focal adhesions and invadopodia, we sought to investigate the role of PTPα in regulating the activity of MMP14-positive plasma membrane protrusions that promote cellular invasion of TNBC cells.

In this study, we define a novel role of PTPα in regulating MMP14 localization to plasma membrane protrusions and in promoting the invasive capacity of TNBC cells. These findings indicate that PTPα plays a central role in mediating breast cancer cell invasion in vivo.

RESULTS

PTPα mediates matrix degradation

PTPα regulates the migratory abilities of fibroblasts (Von Wichert *et al.*, 2003; Zeng *et al.*, 2003; Chen *et al.*, 2006); however, the role of PTPα in cancer cell motility remains relatively unknown. We first used two small-interfering RNA (siRNA) sequences (siα1 and siα2) to transiently knockdown PTPα expression in MDA-MB-231 cells, a TNBC cell line widely used to investigate mechanisms of tumor cell migration and invasion. Both siRNAs were used together to deplete PTPα, and the introduction of siRNA-resistant wild-type PTPα into PTPα-depleted cells rescued the expression of PTPα (Figure 1A). Notably, siRNA-mediated depletion of PTPα did not affect proliferation of the MDA-MB-231 cells (Supplemental Figure S1A). We also confirmed that depleting PTPα using siRNA did not alter the expression of PTPε (Supplemental Figure S1B), a transmembrane protein tyrosine phosphatase that is closely homologous to PTPα and found to activate Src and contribute to tumorigenesis in Neu-induced mammary tumors (Gil-Henn and Elson, 2003; Krueger *et al.*, 1990).

The metastatic cascade is initiated by cancer cells disseminating from the primary tumor and locally invading the ECM and the surrounding tissue before entering the vasculature. We sought to determine if PTPα plays a role in ECM degradation using a matrix

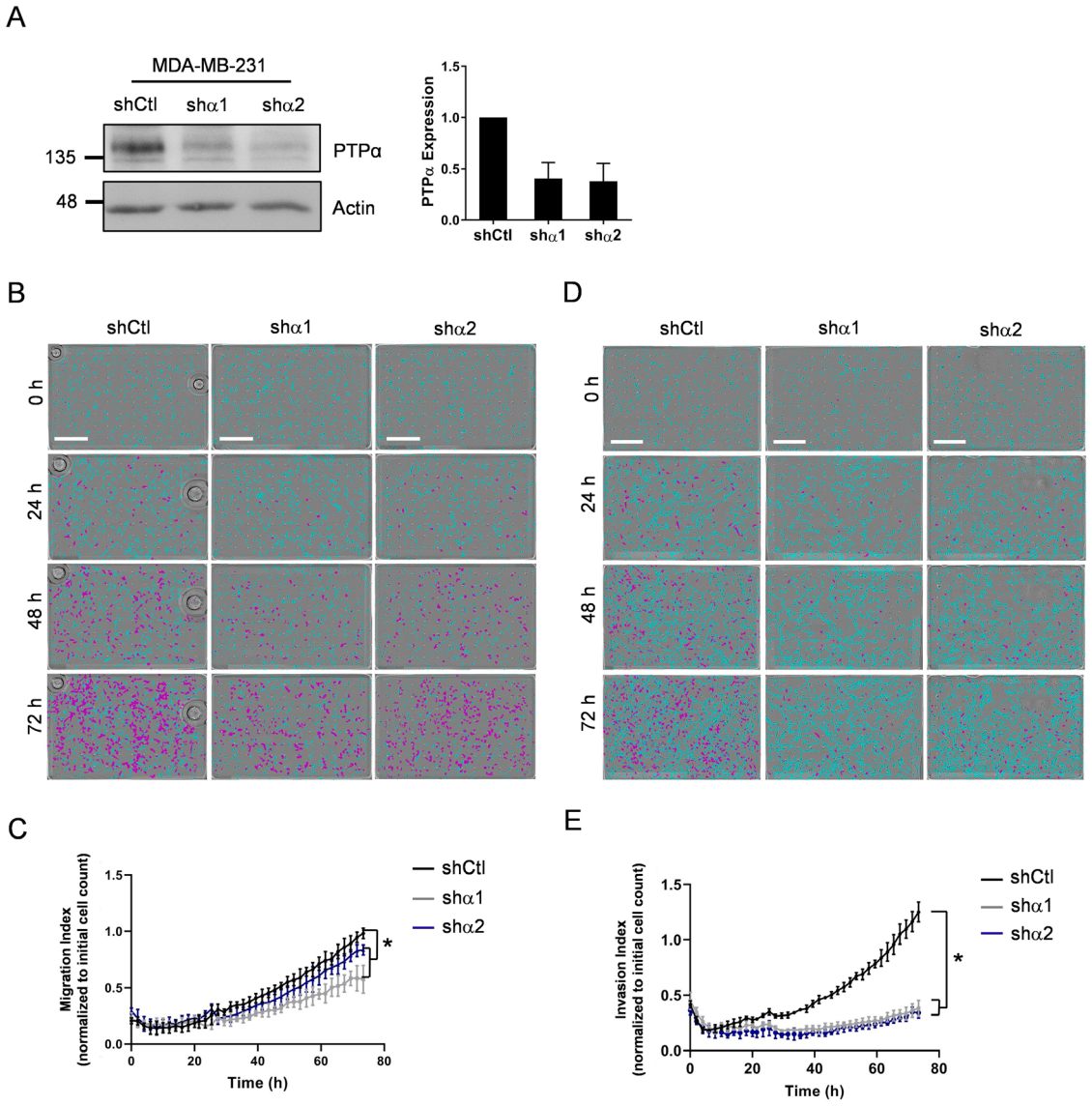

FIGURE 2: PTPα mediates cellular migration and invasion. MDA-MB-231 cells were stably transfected with nontargeting shRNA (shCtl), shRNA-PTPα #1 (shα1), or shRNA-PTPα #2 (shα2). (A) Cell lysates were collected 48 h postseeding and immunoblotted for PTPα and actin. Densitometric quantification of PTPα expression relative to actin was performed using immunoblots of several such cell lysates and is shown in the graph as mean ± SD ($n \geq 3$). (B) Images of cells detected on the top (turquoise) and bottom (purple) surfaces of Transwell inserts at 0, 24, 48, and 72 h of an IncuCyte chemotaxis migration assay. Scale bars = 500 μm. (C) Quantification of migration indices from experiments shown in B are displayed as cell counts normalized to initial cell number. Data are mean ± SD ($n = 3$, $^*p < 0.05$, two-way ANOVA with Tukey's post hoc analysis). (D) Images of the cells detected on the top (turquoise) and bottom (purple) surfaces of Transwell Matrigel inserts at 0, 24, 48, and 72 h of an IncuCyte chemotaxis invasion assay. Scale bars = 500 μm. (E) Quantification of invasion indices from experiments shown in D are displayed as relative cell counts normalized to initial cell number. Data are mean ± SD ($n = 3$, $^*p < 0.05$, two-way ANOVA with Tukey's post hoc analysis).

degradation assay with fluorescently tagged gelatin. Indeed, we observed a decrease in gelatin degradation over a 24 h period upon PTPα knockdown, which was restored by the reexpression of PTPα (Figure 1, B and C). These findings suggest that PTPα is important for ECM degradation and thus may play a role in the initial stages of TNBC cell invasion.

Expression of PTPα is important for TNBC invasion

To further investigate the role of PTPα in cancer cell invasion, two stable MDA-MB-231 cell lines were generated in which PTPα expression was silenced using lentiviral vectors encoding short hairpin RNA (shRNA). MDA-MB-231 cells were transduced with either a nontargeting shRNA control (shCtl) or one of two shRNA-PTPα constructs (shα1 or shα2) targeting unique sequences of the human PTPα gene, with the resulting cell lines referred to as shCtl-231, shα1-231, and shα2-231, respectively. PTPα expression was effectively reduced in shα1-231 cells by 41 ± 15% ($n \geq 3$) and in shα2-231 cells by 38 ± 17% ($n \geq 3$) relative to shCtl-231 cells (Figure 2A).

MDA-MB-231 cell migration and invasion were quantified over time using IncuCyte chemotaxis assays. To determine the role of

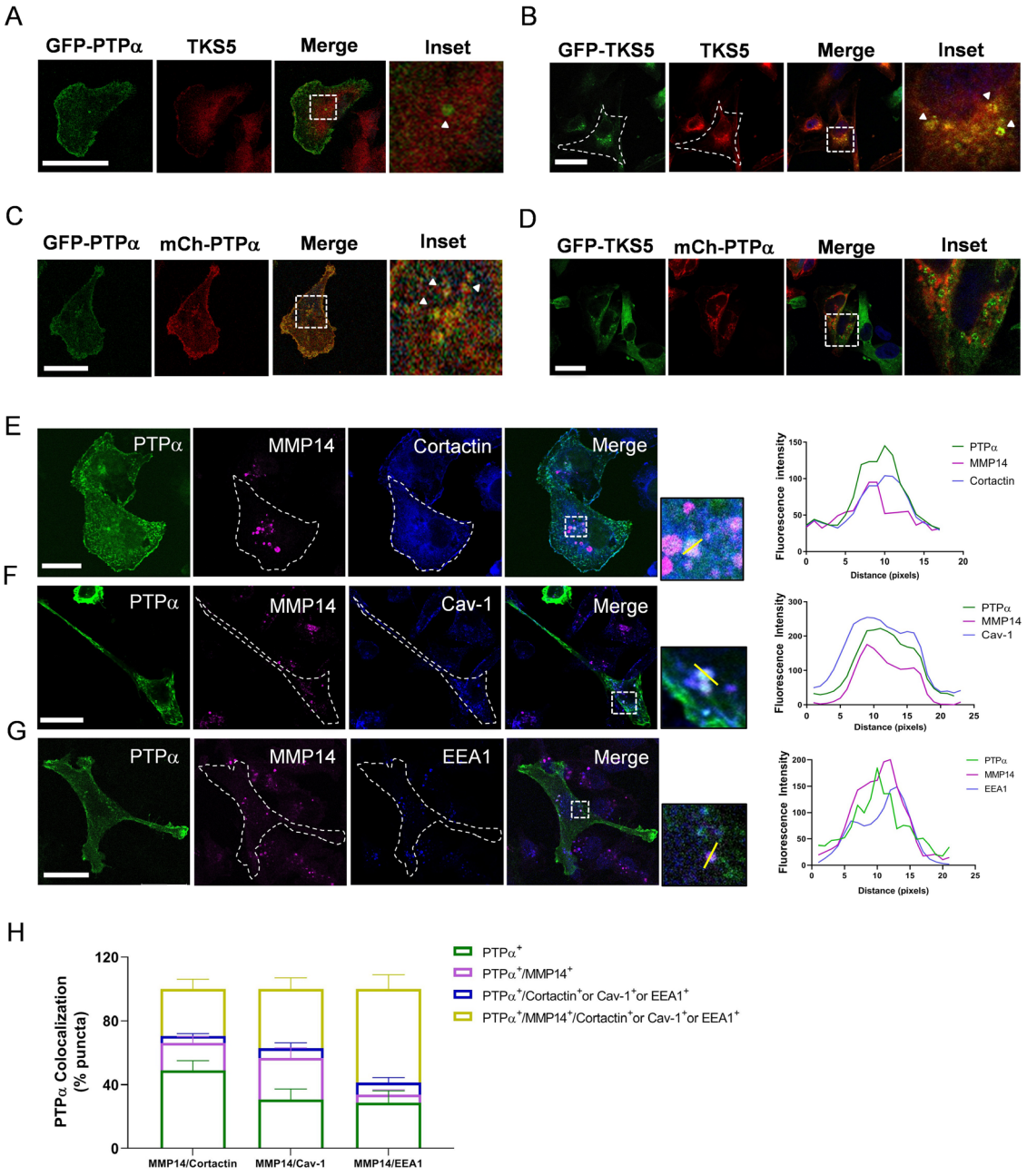

FIGURE 3: PTPα localizes to endosomes but does not localize to TKS5-positive invadopodial structures. (A) Representative images of MDA-MB-231 cells expressing GFP-PTPα and stained for TKS5. (B) Representative images of MDA-MB-231 cells stably expressing GFP-TKS5 and stained for TKS5. (C) Representative images of MDA-MB-231 cells coexpressing GFP-PTPα and mCherry-PTPα. (D) Representative images of MDA-MB-231 cells stably expressing GFP-TKS5 and transiently transfected with mCherry-PTPα. Scale bars = 25 μm. The boxed region is enlarged to the right of the merge image. (E, F, G) Representative images of MDA-MB-231 cells expressing GFP-tagged PTPα and immunofluorescently stained for (E) MMP14 and cortactin, (F) MMP14 and caveolin-1 (cav-1), and (G) MMP14 and early endosome antigen 1 (EEA1). Scale bars = 25 μm. White dotted lines indicate cell outlines. The boxed areas with colocalized signals in the merged images are enlarged to the right. The yellow line across an individual puncta marks where fluorescence pixel intensity was quantified and is displayed in the graphs to the right. (H) Quantification of the percentage of GFP-PTPα expressing puncta that colocalize with MMP14 alone, cortactin/cav-1/EEA1 alone, or MMP14 and one of cortactin/cav-1/EEA1 (n = 22–30 cells).

PTPα in TNBC motility, shCtl-231, shα1-231, and shα2-231 cells were resuspended in either serum-free medium or growth factor–reduced Matrigel to monitor migration or invasion over time, respectively. PTPα depletion resulted in a significant reduction in the ability of MDA-MB-231 cells to migrate through the transwell membrane toward the 10% FBS chemoattractant (Figure 2, B and C). Moreover, MDA-MB-231 cells depleted of PTPα showed an even greater reduction in invasion through the Matrigel (Figure 2, D and E). These data suggest that PTPα expression is important for TNBC cell motility and particularly critical for invasion.

PTPα localizes to endosomal structures but is not present in TKS5-positive invadopodia

The formation of invadopodial structures occurs in three stages: initiation, assembly, and maturation (Artym *et al.*, 2006; Beaty and Condeelis, 2014). The initiation and assembly stages form invadopodial precursor structures, which are non-degradative structures containing actin, cortactin, cofilin, N-WASP, Arp2/3, TKS5, and various other proteins (Eddy *et al.*, 2017). Mature invadopodia are marked by the recruitment and activation of matrix metalloproteinases (MMPs), specifically MMP2, MMP9, and MMP14 (Beaty and Condeelis, 2014). MMP14 is a membrane-bound protein, while both MMP2 and MMP9 are soluble, secreted proteins (Artym *et al.*, 2006; Beaty and Condeelis, 2014; Eddy *et al.*, 2017). The accumulation of proteinases at invadopodia is critical for mediating ECM degradation and cancer cell invasion (Chen and Wang, 1999; Mazzone *et al.*, 2004).

Because PTPα was found to influence ECM degradation and cellular invasion, we sought to determine if PTPα is a component of invadopodia by investigating its colocalization with TKS5, a protein considered a definitive marker of invadopodia (Abram *et al.*, 2003; Seals *et al.*, 2005). GFP-tagged PTPα expressing MDA-MB-231 cells were first stained for TKS5. Immunofluorescence analysis of 20 cells revealed 108 GFP-PTPα positive puncta, of which 105 (97%) were negative for TKS5 (e.g., Figure 3A). We found that very few of the MDA-MB-231 cells expressing GFP-PTPα contained endogenous TKS5-positive invadopodia despite expressing cytoplasmic TKS5. To better visualize TKS5-positive invadopodia, MDA-MB-231 cells stably expressing exogenous GFP-tagged TKS5 were stained with the TSK5 antibody, confirming that this antibody was able to detect TKS5-positive invadopodial structures in TKS5 overexpressing cells and these invadopodia are identified by the GFP-TKS5 (Figure 3B). In subsequent experiments, we found that when the GFP-tagged and mCherry-tagged forms of PTPα were coexpressed, the tagged forms of PTPα colocalized to the membrane and intracellular puncta, validating that the cellular location of either form of exogenous PTPα was not uniquely affected by the tag or plasmid involved (Figure 3C). Finally, to confirm whether PTPα colocalizes with TKS5, mCherry-tagged PTPα was transfected into MDA-MB-231 cells stably expressing GFP-tagged TKS5 before the cells were plated onto gelatin. We found that PTPα–positive puncta were distinct from TKS5-positive structures, indicating that PTPα did not colocalize with TKS5 in invadopodia (Figure 3D). While PTPα-positive puncta formed in close proximity to TKS5-positive invadopodia, only 7.9% (8/101) of GFP-TKS5-positive invadopodia (n = 16 cells) were also positive for mCherry-PTPα (e.g., Figure 3D). Together, these data strongly suggest that PTPα-positive structures are distinct from TKS5-positive invadopodia.

To further characterize the PTPα-positive puncta observed in Figure 3A, we investigated the colocalization of PTPα with cortactin and MMP14, noting that these proteins are present in, but not restricted to, invadopodia. MDA-MB-231 cells transfected with GFP-tagged PTPα were stained for MMP14 and cortactin (Figure 3E, left panel). An analysis of 30 cells revealed 204 GFP-PTPα-positive puncta, and the colocalization of PTPα with cortactin and MMP14 was then analyzed along linear tracks across individual puncta (Figure 3E, right panel). Of these puncta, 48.4% contained PTPα alone, 17.4% were positive for both PTPα and MMP14, 4.3% were positive for both PTPα and cortactin, and 29.5% were positive for PTPα, MMP14, and cortactin together (Figure 3H, left column). Together, these data indicate that PTPα is not present within TKS5-positive invadopodia, but that PTPα is found in cortactin-positive structures that are also positive for MMP14.

Caveolae are a type of lipid raft that regulate endocytic trafficking within the cell (Liu *et al.*, 2002; Poincloux *et al.*, 2009). Given that MMP14 localizes to caveolae (Annabi *et al.*, 2001), that PTPα has been shown to localize to lipid rafts (Maksumova *et al.*, 2005), and that we found that PTPα localizes with non-invadopodial cortactin-positive MMP14-positive structures, we investigated if PTPα is present within caveolae. MDA-MB-231 cells expressing GFP-tagged PTPα were stained for MMP14 and caveolin-1 (cav-1; Figure 3F), and 130 GFP-PTPα-positive puncta were detected in a population of 22 cells. We found that 30.6% of these puncta were positive for PTPα alone, 26.2% for both PTPα and MMP14, 6.1% for both PTPα and cav-1, and 37.1% for PTPα, MMP14, and cav-1 together (Figure 3H, middle column).

Cav-1 also localizes to multiple intracellular compartments and vesicles including the Golgi (Fridolfsson *et al.*, 2014), secretory vesicles, as well as exosomes and endosomes (Mundy *et al.*, 2012; Pelkmans *et al.*, 2004). Based on the size of the observed PTPα/MMP14/cav-1 triple-positive vesicles (>100 nm) in comparison with the known size of caveolae (<100 nm), and since cortactin is also known to colocalize to endosomes (Kaksonen *et al.*, 2000), we stained GFP-PTPα transfected cells with a marker of early endosomes (early endosome antigen 1; EEA1). Indeed, we found that PTPα colocalized with MMP14 in EEA1-positive structures (Figure 3G). More specifically, a total of 78 GFP-positive puncta within 22 cells were analyzed to determine the percentages of MMP14- and EEA1-positive puncta that were also positive for PTPα. We found that 28.6% of the puncta were positive for PTPα alone, 5.2% for both PTPα and MMP14, 7.4% for both PTPα and EEA1, and 58.8% of the puncta exhibited PTPα, MMP14, and EEA1 together (Figure 3H, right column). These analyses indicate that PTPα preferentially localizes to puncta containing both MMP14 and EEA1. Together, these data suggest that PTPα localizes to endosomal structures within the cell.

PTPα depletion inhibits MMP14 localization to plasma membrane protrusions

Because we found that PTPα localizes to early endosome antigen 1, caveolin-1, and MMP14-positive endosomal structures, we then asked if PTPα is involved in trafficking MMP14 to and/or from invadopodial structures. The localization and activity of MMP14 on the plasma membranes of cancer cells is regulated by various mechanisms, including endocytic and exocytic trafficking. Once MMP14 exits the trans-Golgi network (TGN) and reaches the cell surface, the majority of MMP14 is internalized via caveolin- or clathrin-mediated pathways, and MMP14 is first shuttled to early endosomes or shuttled to lysosomes for degradation (Wang *et al.*, 2004). A fraction of the internalized MMP14 residing in non-degradative endosomal compartments in tumor cells is then delivered to invadopodia at the plasma membrane (Gálvez *et al.*, 2004; Poincloux *et al.*, 2009; Williams and Coppolino, 2011; Jacob and Prekeris, 2015; Castro-Castro *et al.*, 2016; Planchon *et al.*, 2018). We investigated if the decrease in matrix degradation observed upon PTPα knockdown is associated with altered levels of MMP14 at the plasma membrane or in invadopodia-like membrane structures.

We found that total MMP14 protein levels were not impacted upon PTPα knockdown, as determined by Western blot analysis (Figure 4A). Using flow cytometry, we did not detect an altered level of membrane-bound MMP14 in PTPα knockdown versus control cells (unpublished data). Given that MMP14 is a plasma membrane–bound protein that may be present within protrusions on the plasma membrane or elsewhere on the cell membrane, we then asked whether PTPα plays a role in the localization of MMP14 to actin- and cortactin-positive plasma membrane protrusions resembling

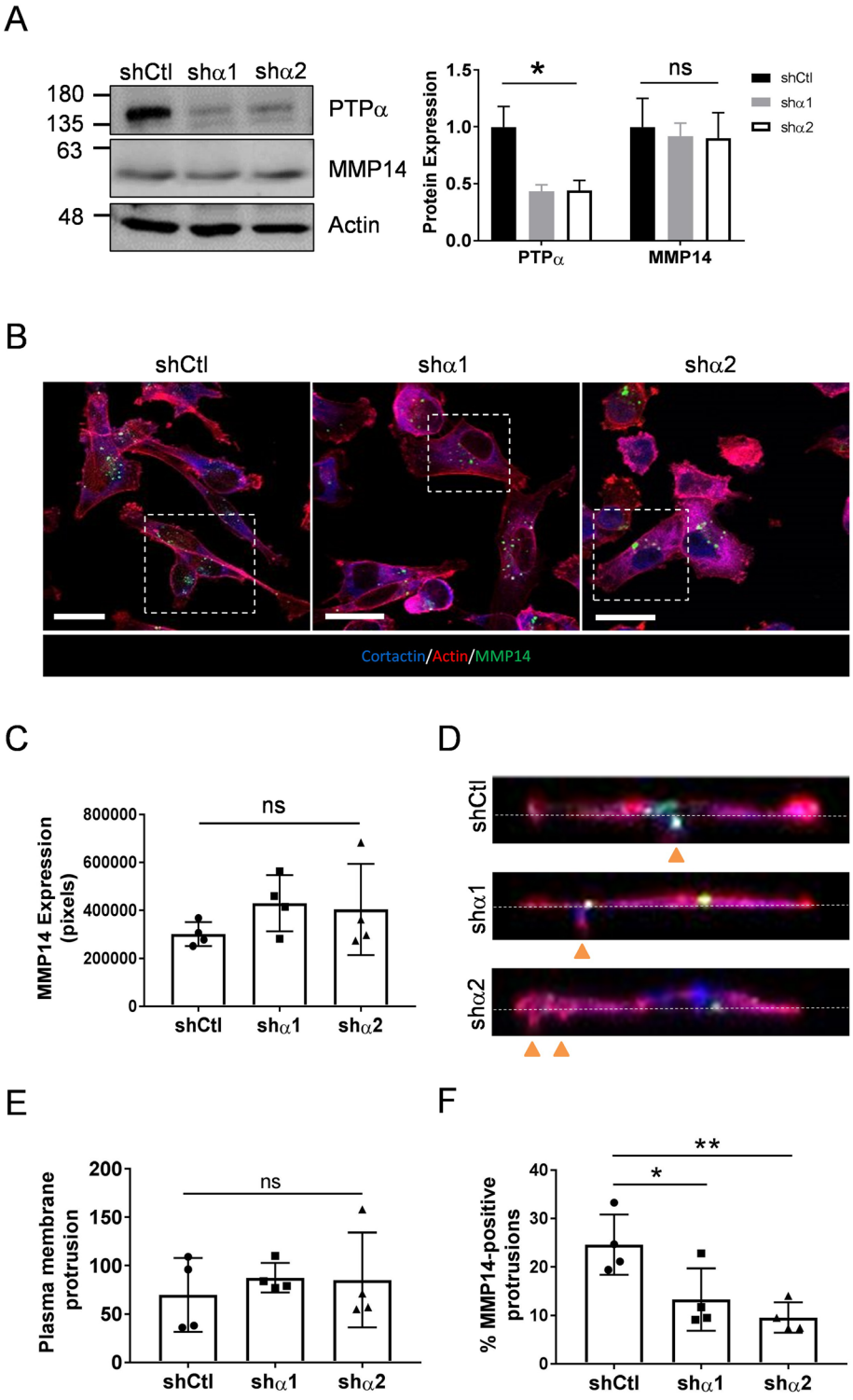

FIGURE 4: PTPα knockdown decreases MMP14 localization to plasma membrane protrusions. (A) Lysates of shCtl, shα1, and shα2 MDA-MB-231 cells were probed for PTPα, MMP14, and actin expression. Densitometric quantification of PTPα and MMP14 expression per unit actin relative to mean control samples was determined from four independent experiments. Data are mean ± SD ($n \geq 3$, $^*p < 0.05$, Student's t test). (B) The shCtl, shα1, and shα2 cells were plated onto Transwell 0.3 μm pore inserts and immunostained for cortactin (blue), actin (red), and MMP14 (green). Scale bars = 25 μm. (C) Total MMP14 expression in cells as shown in B was quantified as mean signal intensity (pixels) using ImageJ. Data are mean ± SD. (D) Representative z-stack images through the areas shown in the dotted boxes in B displaying individual plasma membrane protrusions (indicated with orange arrows). Protrusions containing actin and cortactin are pink; protrusion containing actin, cortactin, and MMP14 are yellow-white, and extend through the pores below the membrane (white dotted line). (E, F) Quantification of (E) the total number of cellular protrusions observed and (F) the percentage of cellular protrusions containing MMP14. Data are mean ± SD. (C, E, F) An average of 145 cells were imaged per cell type ($n = 4$, $^*p < 0.05$, $^{**}p < 0.01$, one-way ANOVA with Tukey's post hoc analysis).

invadopodia. To address this, shCtl-231, shα1-231, and shα2-231 cells were plated onto polycarbonate membranes with 0.3 μm–diameter pores to allow the cells to form plasma membrane protrusions through the pores toward a chemoattractant. Cells were fixed, stained for cortactin/actin/MMP14, and visualized using confocal microscopy (Figure 4B). Consistent with results obtained via immunoblotting, we did not observe a difference in cellular MMP14 expression upon depletion of PTPα (Figure 4C). We then created z-stack images to visualize the plasma membrane structures extending downwards through the pores (Figure 4D; Supplemental Figure S2). Importantly, the z-stack images revealed that the number of protrusions extending through the pores remained similar among equal numbers of control and PTPα knockdown cells (Figure 4E). However, the proportion of plasma membrane protrusions containing MMP14 was significantly lower in cells lacking PTPα (Figure 4F). These results demonstrate that PTPα is important for the localization of MMP14 to plasma membrane protrusions.

PTPα regulates the growth and invasion of TNBC cells into the surrounding mammary fat pad

Our in vitro data demonstrate that PTPα is an important player in the localization of MMP14, ECM degradation, and tumor cell migration and invasion. We next investigated whether PTPα regulates breast cancer cell invasion in vivo. PTPα knockdown was confirmed via immunoblotting (Figure 5A) before implantation of shCtl-231, shα1-231, and shα2-231 cells expressing GFP into the fourth mammary fat pad of immunodeficient mice. We observed nearly a twofold reduction in tumor weight upon PTPα knockdown in comparison with control tumors two weeks after implantation (Figure 5B). We sought to determine if the decrease in tumor weight upon depletion of PTPα was due to disparities in proliferation or apoptosis in vivo, as determined by immunohistochemical staining of Ki67 or

cleaved caspase 3 (CC3), respectively. There was no difference in the fraction of proliferative cells between mice bearing shCtl, shα1, and shα2 tumors (Figure 5, C and D). We did observe a significant increase in the percentage of the CC3-positive area in PTPα knockdown tumors compared with the control tumors (Figure 5, C and E), indicating that reduced PTPα expression correlates with increased in vivo apoptotic signaling. However, depletion of PTPα did not induce apoptotic signaling in vitro, as observed by immunoblotting lysates of cultured cells for PARP cleavage (Supplemental Figure S3), indicating that the shRNA-expressing cells were not apoptotic before implantation and thus suggesting that PTPα may be involved in protecting tumor cells from apoptosis in vivo.

We then analyzed local invasion of shCtl-231, shα1-231, and shα2-231 cells in vivo and observed a striking reduction in the ability of PTPα knockdown tumor cells to invade the surrounding mammary fat pad. We found that control tumors often had diffuse tumor margins that extended several hundred μm away from the primary tumor mass, with invasive tracks of tumor cells extending into the fat tissue (Figure 5F). In contrast, the majority of tumors lacking PTPα had clearly delineated tumor margins with minimal extension into the surrounding fat pad (Figure 5F). The area of the invasive tumor was calculated by subtracting the area of the solid tumor (black dotted line) from the total (i.e., solid and invasive) tumor area (yellow dotted line; Figure 5F). We found a decrease in the total area of shα1 and shα2 MDA-MB-231 tumors compared with control tumors (Figure 5G), consistent with the reduced tumor weights (Figure 5B). Importantly, tumors grown from cells lacking PTPα displayed significantly less invasion into the surrounding mammary fat pad (Figure 5H). Notably, the degree of tumor cell invasion into the mammary fat pad was not associated with overall tumor size, as we observed a wide range of solid and invasive tumor areas between mice (Supplemental Figure S4). These data indicate that tumor cell invasion is not dependent on tumor size and that PTPα knockdown decreases both primary tumor growth and tumor cell invasiveness in vivo.

DISCUSSION

The local invasion of breast cancer cells into surrounding tissue is an important step in breast cancer metastasis that can eventually result in the formation of distant metastases. Finding new and innovative ways to stop cancer cells from infiltrating surrounding healthy tissues is key for preventing the cancer from spreading locally and throughout the rest of the body. Our overall objective was to determine if PTPα is involved in breast cancer cell invasion. In this work, we describe a novel role for PTPα in mediating ECM degradation (Figure 1) and MDA-MB-231 breast cancer cell invasion in vitro (Figure 2) and in vivo (Figure 5). We found that PTPα is a component of early endosome antigen 1, caveolin-1, and MMP14-positive endosomal structures in the cell (Figure 3), and determined that PTPα regulates the localization of MMP14 to plasma membrane protrusions resembling invadopodia (Figure 4). Importantly, we show that stable depletion of PTPα inhibits primary tumor growth and invasion of breast cancer cells into the surrounding mammary fat pad (Figure 5). Together, these data indicate an important role for PTPα in TNBC cell invasion and suggest that inhibition of PTPα in vivo may abrogate further metastasis.

Very few studies have investigated the role of PTPα in cancer progression and metastasis. Ardini *et al.* (2000) reported that PTPα expression varies greatly among tumors; however, high PTPα expression in a subset of ER-positive breast cancer correlates with low-grade tumor status and reduced tumor growth and metastasis. Conversely, high mRNA levels of PTPα correlated with late-stage colorectal carcinoma and with increased squamous-cell lung carcinoma tumors, lymph node metastasis, and depth of tumor invasion (Tabiti *et al.*, 1995; Gu *et al.*, 2017). PTPα has also been shown to regulate colon cancer cellular invasion using an ex vivo chicken chorioallantoic membrane (CAM) assay (Krndija *et al.*, 2010). Therefore, the role of PTPα in the progression of cancer appears to be tissue-specific and thus PTPα may be tumor-promoting or tumor-limiting, depending on the tissue of origin. Our work and others recognize PTPα as a potential oncogene (Zheng *et al.*, 1992; Meyer *et al.*, 2014) and suggest that it may be an attractive drug target for the treatment of TNBC, with the added attributes that PTPα depletion is nonlethal (Ponniah *et al.*, 1999; Su *et al.*, 1999), it is accessible as a transmembrane receptor-type protein (Pallen, 2003), and it functions as an upstream activator of the proto-oncogene Src (Zheng *et al.*, 1992; Ponniah *et al.*, 1999; Su *et al.*, 1999).

Notably, PTPα is closely homologous to PTPε, which can act as an oncogene in certain contexts such as in Neu-induced mammary tumor cells (Gil-Henn and Elson, 2003). Due to the structural and functional similarities between PTPα and PTPε (Krueger *et al.*, 1990), we confirmed that PTPε expression is not altered in MDA-MB-231 cells depleted of PTPα; however, this does not rule out the possibility of some, albeit incomplete, functional compensation by PTPε.

The proteolytic activity of MMP14 at invadopodia is tightly regulated by endocytic/exocytic trafficking mechanisms (Beaty and Condeelis, 2014; Castro-Castro *et al.*, 2016; Poincloux *et al.*, 2009). We found that PTPα within MMP14-positive structures that resemble endosomes (marked by EEA1 and cav-1) and MMP14 expression within plasma membrane protrusions decreased upon PTPα knockdown. We also showed that ECM degradation and cellular invasion were reduced following PTPα depletion with no change in total MMP14 expression. Together, these data raise the possibility that PTPα may be involved in endocytic signaling mechanisms. MMP14 is either expressed homogenously on the plasma membrane of cancer cells, or targeted specifically to invadopodia structures. Several studies have shown that upon MMP14 internalization via endocytosis, a fraction of MMP14 is recycled back to the plasma membrane and distributed to invadopodia structures (Castro-Castro *et al.*, 2016; Monteiro *et al.*, 2013; Poincloux *et al.*, 2009). Among other players, it has been reported that the Rho GTPases RhoA and Cdc42 are critical regulators of MMP14 delivery to invadopodia and ECM degradation (Sakurai-Yageta *et al.*, 2008; Jacob and Prekeris, 2015; Eddy *et al.*, 2017). Previous work from our laboratory has shown that PTPα regulates Cdc42 activation in a variety of signaling and cell contexts, notably including integrin-induced signaling in fibroblasts (Samayawardhena and Pallen, 2008; Wang *et al.*, 2009, 2012; Sun *et al.*, 2012). While the role of PTPα in regulating Rho GTPase signaling in cancer cells remains unknown, perhaps the depletion of PTPα in TNBC cells disrupts Cdc42 activation, thus reducing the accumulation of MMP14 at invadopodia. Rab GTPases, most notably Rab5 and Rab7, are other known negative regulators of MMP14 surface expression (Linder and Scita, 2015). Recently, flotillin-induced endocytosis of plasma membrane-bound MMP14 to Rab5-positive endolysosomes was found to be critical for the subsequent targeted delivery of MMP14 to sites of ECM degradation (Planchon *et al.*, 2018). This raises the question of whether PTPα-MMP14-EEA1-positive endosomes are also involved in flotillin-induced endocytosis of MMP14, and if depletion of PTPα down-regulates flotillin expression, resulting in decreased targeted delivery of MMP14 to invadopodia. Future work is also required to elucidate the precise pathways linking PTPα, caveolin-1, and EEA1 to endocytic trafficking of MMP14 in TNBC cells.

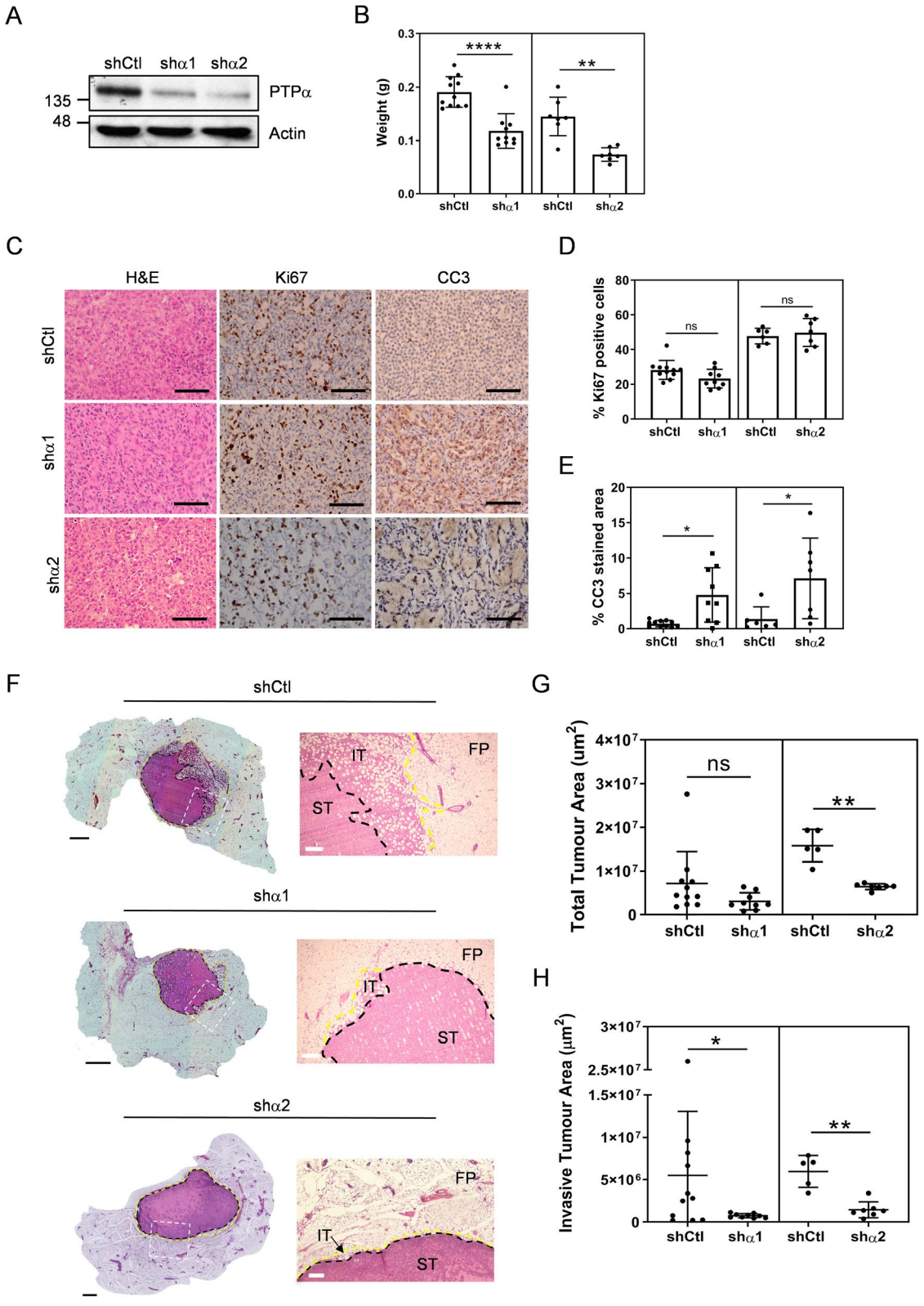

FIGURE 5: Depletion of PTPα induces apoptosis and decreases invasion of breast tumor xenografts. (A) Cell lysates of shCtl, shα1, and shα2 GFP-expressing MDA-MB-231 cells were probed for PTPα and actin expression. (B) MDA-MB-231 tumor cells (1.0×10^6) were orthotopically injected into the fourth mammary fat pads of immunodeficient mice. Total weight (g) of the mammary fat pad and tumor was evaluated 14 d after implantation. (C) Control (shCtl) or PTPα-knockdown (shα1 and shα2) mammary tumors were analyzed via immunohistochemistry (scale bars = 200 μm). Tumors were stained with hematoxylin and eosin (H&E, tumor cell nuclei marker), Ki67 (proliferative cell marker), and cleaved caspase 3 (CC3, apoptotic cell marker). (D, E) Quantification of the percentage of Ki67-positive cells (D) and the percentage of the CC3-positive area (E) within the mammary tumors normalized to total cell number as determined by

In 2012, Wang and McNiven (2012) described a mechanism by which MMP14 is targeted to FAs by associating with a focal adhesion kinase (FAK)-p130Cas complex in pancreatic cancer cell lines. The physical interaction between MMP14 and the FAK-p130Cas complex required for FA-dependent ECM degradation is dependent upon Src-mediated phosphorylation of MMP14 at tyrosine residue 573 on the cytoplasmic tail of MMP14. Previous work in our laboratory identified a role for PTPα in Src-signaling mechanisms that regulate actin stress fiber assembly, FA dynamics, and fibroblast migration (Zeng *et al.*, 2003; Chen *et al.*, 2006; Boivin *et al.*, 2013). Upon integrin stimulation, PTPα dephosphorylates Src at the Tyr^{527} residue to promote Src activation (Zeng *et al.*, 2003; Chen *et al.*, 2006). Active Src associates with FAK and phosphorylates FAK at various tyrosine residues. The Src-FAK complex can then phosphorylate PTPα at Tyr^{789}, identifying PTPα as both an upstream activator and a downstream effector of Src (Zeng *et al.*, 2003; Chen *et al.*, 2006). PTPα-phospho-Tyr^{789} was later shown to bind BCAR3 and subsequently Cas to recruit Cas to FAs, where it can regulate downstream signaling (Sun *et al.*, 2012). Due to this relationship between PTPα and the Src signaling pathway in fibroblasts, it seems plausible that PTPα could act through a similar BCAR3-Cas-Src axis to regulate MMP14 recruitment to plasma membrane structures and influence tumor cell invasion. However, whether Src or other SFKs are involved in the PTPα-mediated regulation of TNBC invasion remains to be elucidated.

Importantly, using an orthotopic xenograft model, we assessed the role of PTPα in mediating TNBC tumor growth and cellular invasion in vivo. We found that tumors lacking PTPα were significantly smaller and exhibited less invasive tumor margins than the control MDA-MB-231 tumors, supportive of our in vitro data. Notably, other groups have shown that depletion of invasion-associated proteins limits tumor growth in vivo. Reduced expression of TKS5, an invadopodia scaffold protein, results in decreased mammary tumor growth accompanied by reduced proliferation and increased apoptosis (Blouw *et al.*, 2008, 2015). Similarly, loss of cortactin and MMP14 profoundly reduced the growth of head and neck squamous cell carcinoma (HNSCC) and squamous cell carcinoma (SCC-1) tumors, respectively (Hotary *et al.*, 2003; Clark *et al.*, 2009). In addition to decreased invasive potential, we also observed an induction of apoptosis in vivo upon the suppression of PTPα in TNBC tumors, which mimics the phenotype observed upon TKS5 depletion. Previous work showed that depletion of PTPα had no significant effect on cellular proliferation or apoptosis, as determined by IHC staining of Her2-positive mammary tumors (Meyer *et al.*, 2014). Interestingly, oligodendrocyte progenitor cells (OPCs) isolated from PTPα-null mouse embryonic brains and cultured in vitro displayed increased proliferation and decreased apoptosis compared with OPCs from WT brains (Wang *et al.*, 2012). Other groups have reported that suppression of PTPα activity induced apoptosis in ER-negative breast cancer and colon cancer cells, but not ER-positive breast cancer cells (Zheng *et al.*, 2008). We found no difference in apoptosis in vitro, but observed increased CC3 expression in tumors formed by PTPα-depleted TNBC cells in vivo, suggesting that PTPα protects tumor cells from apoptosis induced within the solid tumor microenvironment.

Taken together, our data identify a novel relationship between PTPα and MMP14, with PTPα acting as an important mediator of MMP14 localization in breast cancer cells. Our findings also identify PTPα as a potential target to reduce triple-negative breast cancer invasion in vitro and in vivo.

MATERIALS AND METHODS

Cell lines

MDA-MB-231 cells (American Type Culture Collection, ATCC HTB-26) were maintained in DMEM (Hyclone) and supplemented with 10% fetal bovine serum (FBS) and 1% penicillin–streptomycin. GFP-TKS5 expressing MDA-MB-231 cells were a kind gift from Karla Williams (UBC). Cell lines were confirmed to be mycoplasma-free using the a LookOut Mycoplasma PCR detection kit (Sigma-Aldrich, Cat. No. MP0035).

Antibodies

Rabbit anti-PTPα antiserum 2205 has been described previously (Lim *et al.*, 1998; Chen *et al.*, 2006). Primary antibodies against the following proteins were used: anti-PTPε (Abcam, Cat. No. ab126788), anti-actin (Sigma, Cat. No. A2066), anti-cortactin (Millipore, Cat. No. 05-180), anti-MT1-MMP (MMP14; Millipore, Cat. No. ab38898), anti-TKS5 (Santa Cruz, Cat. No. sc-30122), anti-EEA1 (Abcam, Cat. No. ab2900), and anti-PARP (Cell Signaling Technology, Cat. No. 9542). Secondary antibodies used were anti-rabbit IgG peroxidase conjugate (Sigma, Cat. No. A4914), anti-mouse IgG peroxidase antibody (Sigma, Cat. No. A4416), Alexa Fluor 594-conjugated to phalloidin (ThermoFisher, Cat. No. A12381), Alexa Fluor 488-conjugated goat anti-mouse IgG (Molecular Probes, Cat. No. A11001), Alexa Fluor 647-conjugated goat anti-rabbit IgG (Life Technologies, Cat. No. A21245), Alexa Fluor 594-conjugated goat anti-mouse IgG (Life Technologies, Cat. No. A11032), and Alexa Fluor 405-conjugated goat anti-mouse IgG (Life Technologies, Cat. No. A31553). Control normal mouse (Cat. No. 12-371) and normal rabbit (Cat. No. 12-370) IgG antibodies were purchased from Millipore.

siRNA transfection and plasmids

MDA-MB-231 cells were transfected with siRNA to transiently knock down PTPα. Sequences for the siRNAs used to target PTPα are as follows: siα1, 5′-GCAUUACAAUUUCACCAAA-3′; siα2, 5′-CGGCAGAACCAGUUAAAGA-3′ (Thermo Scientific, J-004519-06 and J-004519-08, respectively). Control nontargeting siRNA was purchased from Dharmacon. Cells were transfected with 20 nM siRNA using Lipofectamine RNAiMAX reagent (Invitrogen) and grown for 48 h before further experimentation. The pXJ41-neo-hPTPα siRNA-resistant plasmid was cotransfected with siRNA using Lipofectamine-2000 reagent (Invitrogen) to restore wild-type PTPα expression, and cells were grown for 48 h before further experimentation. The pXJ41-neo-EGFP-PTPα and pXJ41-neo-mCherry-PTPα plasmids were generated by replacing the PacI-flanked nucleotide sequence encoding a VSVG tag (located in the extracellular

H&E staining (n = 6–11 shCtl tumors, n = 9 shα1 tumors, n = 7 shα2 tumors,*$p < 0.05$, Student's t test). (F) Left: representative sections of control (shCtl) or PTPα-knockdown (shα1 and shα2) mammary tumors and fat pads stained with H&E (yellow dotted line, total tumor area; black dotted line, solid tumor area; scale bar, 500 μm). Right: higher-magnification images of the white boxed areas (ST, solid tumor; IT, invasive tumor; FP, fat pad; black dotted line, solid tumor margin; yellow dotted line, total tumor margin; scale bars = 200 μm). (G, H) Quantification of (G) total and (H) invasive tumor area (μm^2) in H&E sections from 5–11 shCtl, 9 shα1, and 7 shα2 tumors per group (*$p < 0.05$, Student's t test).

domain of PTPα) in the plasmid pXJ41-neo-VSVG-PTPα (Bhandari *et al.*, 1998) with PCR-generated PacI-flanked sequences encoding EGFP or mCherry. These plasmids were transfected into MDA-MB-231 cells with Lipofectamine-2000 reagent (Invitrogen) according to the manufacturer's instructions.

Generation of stable cell lines

For stable depletion of PTPα in MDA-MB-231 cells, shRNA constructs were transduced using lentivirus per the manufacturer's instructions. Two shRNA-expressing constructs against PTPα and one control sequence were purchased from Sigma Aldrich (Cat. No. SHCLNV-NM_002836, Cat. No. SHCLNV-NM_002839, and Cat. No. shC005V, respectively). Briefly, MDA-MB-231 cells were seeded at a density of 9000 cells per well in a 96-well plate. After 24 h, 8 μg/ml hexadimethrine and the viral particles at a multiplicity of infection (MOI) of 1 per well were added. Transduced cells were selected using 0.5 μg/ml puromycin and maintained in puromycin-containing culture medium.

IncuCyte chemotaxis migration and invasion assays

In brief, control and shRNA-expressing MDA-MB-231 cells were serum-starved overnight before being resuspended in serum-free medium (migration assay) or 5.0 mg/ml Matrigel (Corning, Cat. No. 356231, invasion assay) and plated into a ClearView 96-well cell migration plate (Essen Biosciences, Cat. No. 4582). Chemotactic migration and invasion were monitored at 2 h intervals for 72 h using IncuCyte analysis software (Essen BioScience, Ann Arbor, MI, USA). Cellular migration and invasion were quantified as changes in cell count over time normalized to the initial cell counts (0 h).

Immunoblotting

MDA-MB-231 cells were lysed with RIPA buffer (50 mM Tris Cl pH 7.4, 150 mM NaCl, 1 mM EDTA, 1% Nonidet P-40, 0.5% NaDOC, 10 μg/μl Aprotinin, 10 μg/μl Leupeptin, 1 mM phenylmethylsulfonyl fluoride, and 2 mM sodium orthovanadate) and total protein concentration was determined using BioRad Protein Assay Dye. The cell lysates were prepared using reducing conditions, and 20 μg (PTPα, MMP14) or 30 μg (PARP) of protein was resolved by SDS–PAGE. The proteins were transferred to polyvinylidene difluoride (PVDF) membranes, blocked in 3% BSA–PBS with 0.1% Tween-20, and immunoblotted with the indicated antibodies. The immunoblots were visualized using ECL detection methods.

Matrix degradation assay

This protocol was adapted from Martin *et al.* (2012). In brief, 13-mm glass coverslips were washed in 20% H_2SO_4 for 30 min and washed with dH_2O before use. The coverslips were placed in wells of a sterile 24-well plate, coated with 50 μg/ml Poly-L-Lysine for 20 min at room temperature (RT), washed with phosphate-buffered saline (PBS), incubated in 0.5% glutaraldehyde for 15 min on ice, and then washed with PBS. Each coverslip was incubated for 10 min in 100 μl of 125 μg/ml Oregon Green 488-conjugated gelatin (Molecular Probes) at RT. The excess gelatin was then removed, and the coverslips were washed in 5 mg/ml sodium borohydride for 15 min, washed with PBS, and incubated in 70% ethanol for 30 min at RT. The coverslips were washed with sterile PBS and 7.5×10^4 cells were added per well. After 24 h, the cells were fixed with 4% PFA and permeabilized with 0.2% Triton X-100 in PBS for immunofluorescent analysis. Approximately 90 to 120 cells were imaged (~15 FOVs) at 63× magnification per condition per experiment. Gelatin degradation was quantified using ImageJ. ECM degradation was analyzed by quantifying the area of gelatin degradation as a percentage of the total area per field of view and normalized to the number of cells per field.

Immunofluorescence

Glass coverslips were coated with 1 mg/ml gelatin, and 7.5×10^4 MDA-MB-231 cells were seeded per coverslip in a 24-well plate for 24 h. The cells were fixed with 4% PFA for 15 min, washed three times in PBS, permeabilized in 0.2% Triton X-100/PBS for 10 min, and blocked with 3% bovine serum albumin (BSA) in 0.2% Triton X-100/PBS for 1 h at RT. The blocking solution was removed, and the samples were incubated with primary antibodies overnight at 4°C and with secondary antibodies and/or phalloidin for 2 h at RT. Post washes, the coverslips were mounted with mounting medium with or without DAPI (Molecular Probes). For colocalization analysis, MDA-MB-231 cells were transfected with either mCherry-PTPα or GFP-PTPα, stained with comarkers, imaged at 100× magnification using a Leica SP5 confocal microscope, and analyzed using ImageJ software. The percentage of colocalization was quantified across 22–30 PTPα-positive cells that formed between 78 and 204 PTPα-positive puncta in total. To visualize MMP14 localization to plasma membrane protrusions, cells were seeded (2.5×10^4) onto 0.3 μm membranes (Costar) in serum-free medium. The bottom chamber was filled with medium containing 10% FBS as the chemoattractant, and the plasma membrane protrusions could extend overnight at 37°C/5% CO_2. Cells were fixed onto the membrane, permeabilized, blocked, and stained as described above.

Orthotopic xenograft tumor model

Female immunodeficient mice aged 8–19 wk [NSG (NOD scid gamma) mice used for shCtl vs. shα1 experiments and NRG (NOD.Cg-Rag^{1tm1Mom} Il2rg^{tm1Wjl}/SzJ) mice used for shCtl vs. shα2 experiments] were bred in-house in the Animal Resource Centre at the BC Cancer Research Centre under specific pathogen-free conditions. Either shCtl, shα1, or shα2 GFP-expressing MDA-MB-231 (1.0×10^6) cells were resuspended in complete culture medium and mixed with an equal volume of high-concentration Matrigel (Corning). Mice were anesthetized by 2% isoflurane inhalation and randomly divided into two groups, and the cell–Matrigel mixture was injected into the fourth mammary fat pad in a total volume of 100 μl. Tumors and surrounding fat pads were harvested 2 wk post-implantation for further analysis. Animal experiments were performed in accordance with Institution and Canadian Council on Animal Care guidelines.

Immunohistochemistry

The mammary fat pads containing tumors were isolated, weighed, and then fixed in 10% formalin. The samples were paraffin-embedded, processed, and stained with hematoxylin/eosin (H&E; Biocare, Cat. No. CATHE), Ki67 (Springer Bioscience, Cat. No. M3062), and/or cleaved caspase-3 (Cell Signaling, Cat. No. 9661S) by the BC Cancer Agency's Molecular and Cellular Immunology Core Facility (Victoria, BC, Canada). Images were captured using a Zeiss Axioplan 2 microscope and Northern Eclipse software and processed using Fiji (Fiji is Just ImageJ) software. H&E staining was used to differentiate mammary fat pad cells from tumor cells, and the density of H&E stained nuclei was used to distinguish between the solid tumor mass and the invasive front of the tumor. The average area of invasive tumor (μm^2) was calculated as the difference between the total tumor area and the solid tumor area in five step sections (100 μm apart) per mouse. The expression of proliferation and apoptosis markers (Ki67 and CC3, respectively) were quantified from three randomly imaged FOVs (one section per mouse)

using Fiji and normalized to total tumor cell number in the section as determined by quantification of hematoxylin staining.

Statistical Analysis

Statistical comparisons were made using unpaired, two-tailed Student's *t* tests with Welch's correction. When more than two groups were analyzed, either a one-way (single time point) or a two-way (time course analysis) ANOVA was performed. Significance was defined as $p < 0.05$ and all data represent at least three independent experiments. Experimental values are presented as the mean ± SD (SD).

ACKNOWLEDGMENTS

We would like to thank members of the Pallen and Bennewith labs for helpful discussions and input. We are grateful to H. T. Le for generation of the mCherry- and EGFP-tagged PTPα plasmids and to members of K. Williams's lab (UBC) for supplying the GFP-TKS5 expressing MDA-MB-231 cells. We wish to acknowledge the BC Cancer Agency's Molecular and Cellular Immunology Core Facility, Victoria, BC, Canada for their help with processing and staining the breast tumor xenograft tissues. This work was supported by the Canadian Institutes of Health Research (CIHR; PJT-148692 to CJP). L.R.D. and B.J.W. are scholars in the Terry Fox Foundation Initiative for Strategic Training in Transdisciplinary Radiation Science for the 21st Century (STARS21). L.R.D. was also supported by a CIHR Fredrick Banting and Charles Best Canadian Graduate Scholarship Master's award and a Michael Cuccione Childhood Cancer Foundation Graduate Studentship. B.J.W. was supported by a Doctoral Research Award from CIHR. K.L.B. is a Michael Smith Foundation of Health Research Biomedical Research Scholar.

REFERENCES

Abram CL, Seals DF, Pass I, Salinsky D, Maurer L, Roth TM, Courtneidge SA (2003). The adaptor protein fish associates with members of the ADAMs family and localizes to podosomes of Src-transformed cells. J Biol Chem 278, 16844–16851.

Al-Mahmood S, Sapiezynski J, Garbuzenko OB, Minko T (2018). Metastatic and triple-negative breast cancer: challenges and treatment options. Drug Deliv Transl Res 8, 1483–1507.

Annabi B, Lachambre M-P, Bousquet-Gagnon N, Page M, Gingras D, Beliveau R (2001). Localization of membrane-type 1 matrix metalloproteinase in caveolae membrane domains. Biochem J 353, 547–553.

Ardini E, Agresti R, Tagliabue E, Greco M, Aiello P, Yang L-T, Ménard S, Sap J (2000). Expression of protein tyrosine phosphatase alpha (RPTPα) in human breast cancer correlates with low tumor grade and inhibits tumor cell growth in vitro and in vivo. Oncogene 19, 4979–4987.

Artym VV, Zhang Y, Seillier-Moiseiwitsch F, Yamada KM, Mueller SC (2006). Dynamic interactions of cortactin and membrane type 1 matrix metalloproteinase at invadopodia: defining the stages of invadopodia formation and function. Cancer Res 66, 3034–3043.

Beaty BT, Condeelis J (2014). Digging a little deeper: The stages of invadopodium formation and maturation. Eur J Cell Biol 93, 438–444.

Bhandari V, Lim KL, Pallen CJ (1998). Physical and functional interactions between receptor-like protein-tyrosine phosphatase alpha and p59fyn. J Biol Chem 273, 8691–8698.

Blouw B, Patel M, Iizuka S, Abdullah C, You WK, Huang X, Li J-L, Diaz B, Stallcup WB, Courtneidge SA (2015). The invadopodia scaffold protein Tks5 is required for the growth of human breast cancer cells in vitro and in vivo. PLoS One 10, e0121003.

Blouw B, Seals DF, Pass I, Diaz B, Courtneidge SA (2008). A role for the podosome/invadopodia scaffold protein Tks5 in tumor growth in vivo. Eur J Cell Biol 87, 555–567.

Boivin B, Chaudhary F, Dickinson BC, Haque A, Pero SC, Chang CJ, Tonks NK (2013). Receptor protein-tyrosine phosphatase α regulates focal adhesion kinase phosphorylation and ErbB2 oncoprotein-mediated mammary epithelial cell motility. J Biol Chem 288, 36926–36935.

Castro-Castro A, Marchesin V, Monteiro P, Lodillinsky C, Rossé C, Chavrier P (2016). Cellular and molecular mechanisms of MT1-MMP-dependent cancer cell invasion. Annu Rev Cell Dev Biol 32, 555–576.

Chan KT, Cortesio CL, Huttenlocher A (2009). FAK alters invadopodia and focal adhesion composition and dynamics to regulate breast cancer invasion. J Cell Biol 185, 357–370.

Chen M, Chen SC, Pallen CJ (2006). Integrin-induced tyrosine phosphorylation of protein-tyrosine phosphatase-alpha is required for cytoskeletal reorganization and cell migration. J Biol Chem 281, 11972–11980.

Chen W, Wang J (1999). Specialized surface protrusions of invasive cells, invadopodia and lamellipodia, have differential MT1-MMP, MMP-2, and TIMP-2 localization. Ann N Y Acad Sci 878, 361–371.

Clark ES, Brown B, Whigham AS, Kochaishvili A, Yarbrough WG, Weaver AM (2009). Aggressiveness of HNSCC tumors depends on expression levels of cortactin, a gene in the 11q13 amplicon. Oncogene 28, 431–444.

Canadian Cancer Statistics Advisory Committee (2019). Canadian Cancer Statistics. 2019.

Dawson SJ, Provenzano E, Caldas C (2009). Triple negative breast cancers: clinical and prognostic implications. Eur J Cancer 45, 27–40.

Eddy RJ, Weidmann MD, Sharma VP, Condeelis JS (2017). Tumor cell invadopodia: Invasive protrusions that orchestrate metastasis. Trends Cell Biol 27, 595–607.

Fridolfsson HN, Roth DM, Insel PA, Patel HH (2014). Regulation of intracellular signaling and function by caveolin. FASEB J 28, 3823–3831.

Frittoli E, Palamidessi A, Disanza A, Scita G (2011). Secretory and endo/exocytic trafficking in invadopodia formation: The MT1-MMP paradigm. Eur J Cell Biol 90, 108–114.

Gálvez BG, Matías-Román S, Yáñez-Mó M, Vicente-Manzanares M, Sánchez-Madrid F, Arroyo AG (2004). Caveolae are a novel pathway for membrane-type 1 matrix metalloproteinase traffic in human endothelial cells. Mol Biol Cell 15, 678–687.

Gil-Henn H, Elson A (2003). Tyrosine phosphatase-ε activates Src and supports the transformed phenotype of Neu-induced mammary tumor cells. J Biol Chem 278, 15579–15586.

Gligorijevic B, Wyckoff J, Yamaguchi H, Wang Y, Roussos ET, Condeelis J (2012). N-WASP-mediated invadopodium formation is involved in intravasation and lung metastasis of mammary tumors. J Cell Sci 125, 724–734.

Gu Z, Fang X, Li C, Chen C, Liang G, Zheng X, Fan Q (2017). Increased PTPRA expression leads to poor prognosis through c-Src activation and G1 phase progression in squamous cell lung cancer. Int J Oncol 51, 489–497.

Hotary KB, Allen ED, Brooks PC, Datta NS, Long MW, Weiss SJ (2003). Membrane type I matrix metalloproteinase usurps tumor growth control imposed by the three-dimensional extracellular matrix. Cell 114, 33–45.

Jacob A, Prekeris R (2015). The regulation of MMP targeting to invadopodia during cancer metastasis. Front Cell Dev Biol 3, 1–4.

Kaksonen M, Peng HB, Rauvala K (2000). Association of cortactin with dynamic actin in lamellipodia and on endosomal vesicles. J Cell Sci 113, 4421–4426.

Krndija D, Schmid H, Eismann J-L, Lother U, Adler G, Oswald F, Seufferlein T, von Wichert G (2010). Substrate stiffness and the receptor-type tyrosine-protein phosphatase alpha regulate spreading of colon cancer cells through cytoskeletal contractility. Oncogene 29, 2724–2738.

Krueger NX, Streuli M, Saito H (1990). Structural diversity and evolution of human receptor-like protein tyrosine phosphatases. EMBO J 9, 3241–3252.

Leong HS, Robertson AE, Stoletov K, Leith SJ, Chin CA, Chien AE, Hague MN, Ablack A, Carmine-Simmen K, McPherson VA, *et al.* (2014). Invadopodia are required for cancer cell extravasation and are a therapeutic target for metastasis. Cell Rep 8, 1558–1570.

Lim KL, Kolatkar PR, Peng Ng K, Hoe Ng C, Pallen CJ (1998). Interconversion of the kinetic identities of the tandem catalytic domains of receptor-like protein-tyrosine phosphatase PTP alpha by two point mutations is synergistic and substrate-dependent. J Biol Chem 273, 28986–28993.

Linder S, Scita G (2015). RABGTPases in MT1-MMP trafficking and cell invasion: physiology versus pathology. Small GTPases 6, 145–152.

Liu P, Rudick M, Anderson RGW. (2002). Multiple functions of caveolin-1. J Biol Chem 277, 41295–41298.

Lohmer LL, Kelley LC, Hagedorn EJ, Sherwood DR (2014). Invadopodia and basement membrane invasion in vivo. Cell Adh Migr 8, 246–255.

Mader CC, Oser M, Magalhaes MAO, Bravo-Cordero JJ, Condeelis J, Koleske AJ, Gil-Henn H. (2011). An EGFR-Src-Arg-cortactin pathway mediates functional maturation of invadopodia and breast cancer cell invasion. Cancer Res 71, 1730–1741.

Maksumova L, Le HT, Muratkhodjaev F, Davidson D, Andre´ Veillette A, Pallen CJ (2005). Protein tyrosine phosphatase αregulates Fyn activity

and Cbp/PAG phosphorylation in thymocyte lipid rafts. J Immunol 175, 7947–7956.
Martin KH, Hayes KE, Walk EL, Ammer AG, Markwell SM, Weed SA (2012). Quantitative measurement of invadopodia-mediated extracellular matrix proteolysis in single and multicellular contexts. J Vis Exp e4119.
Mazzone M, Baldassarre M, Beznoussenko G, Giacchetti G, Cao J, Zucker S, Luini A, Buccione R (2004). Intracellular processing and activation of membrane type 1 matrix metalloprotease depends on its partitioning into lipid domains. J Cell Sci 117, 6275–6287.
Meyer DS, Aceto N, Sausgruber N, Brinkhaus H, Müller U, Pallen CJ, Bentires-Alj M (2014). Tyrosine phosphatase PTPα contributes to HER2-evoked breast tumor initiation and maintenance. Oncogene 33, 398–402.
Monteiro P, Rossé C, Castro-Castro A, Irondelle M, Lagoutte E, Paul-Gilloteaux P, Desnos C, Formstecher E, Darchen F, Perrais D, *et al.* (2013). Endosomal WASH and exocyst complexes control exocytosis of MT1-MMP at invadopodia. J Cell Biol 203, 1063–1079.
Mundy DI, Li WP, Luby-Phelps K, Anderson RGW. (2012). Caveolin targeting to late endosome/lysosomal membranes is induced by perturbations of lysosomal pH and cholesterol content. Mol Biol Cell 23, 864–880.
Murphy DA, Courtneidge SA (2011). The "ins" and "outs" of podosomes and invadopodia: characteristics, formation and function. Nat Rev Mol Cell Biol 12, 413–426.
Pallen CJ (2003). Protein tyrosine phosphatase alpha (PTP alpha): a Src family kinase activator and mediator of multiple biological effects. Curr Top Med Chem 3, 831–835.
Paterson EK, Courtneidge SA (2018). Invadosomes are coming: new insights into function and disease relevance. FEBS J 285, 8–27.
Pelkmans L, Bürli T, Zerial M, Helenius A (2004). Caveolin-stabilized membrane domains as multifunctional transport and sorting devices in endocytic membrane traffic. Cell 118, 767–780.
Planchon D, Rios Morris E, Genest M, Comunale F, Vacher S, Bièche I, Denisov EV, Tashireva LA, Perelmuter VM, Linder S, *et al.* (2018). MT1-MMP targeting to endolysosomes is mediated by upregulation of flotillins. J Cell Sci 131, jcs218925.
Poincloux R, Lizárraga F, Chavrier P (2009). Matrix invasion by tumour cells: a focus on MT1-MMP trafficking to invadopodia. J Cell Sci 122, 3015–3024.
Ponniah S, Wang DZ, Lim KL, Pallen CJ (1999). Targeted disruption of the tyrosine phosphatase PTPalpha leads to constitutive downregulation of the kinases Src and Fyn. Curr Biol 9, 535–538.
Revach O-Y, Geiger B (2014). The interplay between the proteolytic, invasive, and adhesive domains of invadopodia and their roles in cancer invasion. Cell Adh Migr 8, 215–225.
Sakurai-Yageta M, Recchi C, Le Dez G, Sibarita JB, Daviet L, Camonis J, D'Souza-Schorey C, Chavrier P. (2008). The interaction of IQGAP1 with the exocyst complex is required for tumor cell invasion downstream of Cdc42 and RhoA. J Cell Biol 181, 985–998.
Samayawardhena LA, Pallen CJ (2008). Protein-tyrosine phosphatase alpha regulates stem cell factor-dependent c-Kit activation and migration of mast cells. J Biol Chem 283, 29175–29185.
Scully OJ, Bay B-H, Yip G, Yu Y (2012). Breast cancer metastasis. Cancer Genomics Proteomics 9, 311–320.
Seals DF, Azucena EF, Pass I, Tesfay L, Gordon R, Woodrow M, Resau JH, Courtneidge SA (2005). The adaptor protein Tks5/Fish is required for podosome formation and function, and for the protease-driven invasion of cancer cells. Cancer Cell 7, 155–165.
Spinardi L, Rietdorf J, Nitsch L, Bono M, Tacchetti C, Way M, Marchisio PC (2004). A dynamic podosome-like structure of epithelial cells. Exp Cell Res 295, 360–374.
Su J, Muranjan M, Sap J (1999). Receptor protein tyrosine phosphatase alpha activates Src-family kinases and controls integrin-mediated responses in fibroblasts. Curr Biol 9, 505–511.
Sun G, Cheng SYS, Chen M, Lim CJ, Pallen CJ. (2012). Protein tyrosine phosphatase α phosphotyrosyl-789 binds BCAR3 to position Cas for activation at integrin-mediated focal adhesions. Mol Cell Biol 32, 3776–3789.
Tabiti K, Smith DR, Goh H-S, Pallen CJ (1995). Increased mRNA expression of the receptor-like protein tyrosine phosphatase α in late stage colon carcinomas. Cancer Lett 93, 239–248.
Von Wichert G, Jiang G, Kostic A, De Vos K, Sap J, Sheetz MP (2003). RPTP-acts as a transducer of mechanical force on v/3-integrin-cytoskeleton linkages. J Cell Biol 161, 143–153.
Wang PS, Wang J, Xiao ZC, Pallen CJ (2009). Protein-tyrosine phosphatase α acts as an upstream regulator of Fyn signaling to promote oligodendrocyte differentiation and myelination. J Biol Chem 284, 33692–33702.
Wang PS, Wang J, Zheng Y, Pallens CJ (2012). Loss of protein-tyrosine phosphatase α (PTPα) increases proliferation and delays maturation of oligodendrocyte progenitor cells. J Biol Chem 287, 12529–12540.
Wang X, Ma D, Keski-Oja J, Pei D (2004). Co-recycling of MT1-MMP and MT3-MMP through the trans-Golgi network: identification of DKV582 as a recycling signal. J Biol Chem 279, 9331–9336.
Wang Y, McNiven MA (2012). Invasive matrix degradation at focal adhesions occurs via protease recruitment by a FAK-p130Cas complex. J Cell Biol 196, 375–385.
Williams KC, Cepeda MA, Javed S, Searle K, Parkins KM, Makela AV, Hamilton AM, Soukhtehzari S, Kim Y, Tuck AB, *et al.* (2019). Invadopodia are chemosensing protrusions that guide cancer cell extravasation to promote brain tropism in metastasis. Oncogene 38, 3598–3615.
Williams KC, Coppolino MG (2011). Phosphorylation of membrane type 1-matrix metalloproteinase (MT1-MMP) and its vesicle-associated membrane protein 7 (VAMP7)-dependent trafficking facilitate cell invasion and migration. J Biol Chem 286, 43405–43416.
Yamaguchi H, Takeo Y, Yoshida S, Kouchi Z, Nakamura Y, Fukami K (2009). Lipid rafts and caveolin-1 are required for invadopodia formation and extracellular matrix degradation by human breast cancer cells. Cancer Research 69, 8594–8602.
Zeng L, Si X, Yu W-P, Le HT, Ng KP, Teng RMH, Ryan K, Wang DZ-M, Ponniah S, Pallen CJ. (2003). PTP alpha regulates integrin-stimulated FAK autophosphorylation and cytoskeletal rearrangement in cell spreading and migration. J Cell Biol 160, 137–146.
Zheng X, Resnick RJ, Shalloway D (2008). Apoptosis of estrogen-receptor negative breast cancer and colon cancer cell lines by PTP alpha and src RNAi. Int J Cancer 122, 1999–2007.
Zheng XM, Wang Y, Pallen CJ (1992). Cell transformation and activation of pp60 c-src by overexpression of a protein tyrosine phosphatase. Nature 359, 336–339.